Available online at www.sciencedirect.com
SCIENCE DIRECT®
ELSEVIER
Earth and Planetary Science Letters xx (2005) xxx–xxx
EPSL
www.elsevier.com/locate/epsl

Slab dip vs. lithosphere age: No direct function

Claudio Cruciani [a], Eugenio Carminati [a,b,*], Carlo Doglioni [a]

[a] *Department of Earth Sciences, University of Roma 'La Sapienza', Italy*
[b] *Istituto di Geologia Ambientale e Geoingegneria - CNR, Roma, Italy*

Received 15 March 2005; received in revised form 26 July 2005; accepted 26 July 2005

Editor: S. King

Abstract

One paradigm of subduction relates the dip of the slab to the buoyancy of the downgoing lithosphere along subduction zones, with the negative buoyancy proportional to the age of the oceanic lithosphere. We measured the dip of the slab down to depths of 250 km along 164 sections crossing 13 subduction zones and compared it with the age of the subducting oceanic lithosphere both at the trench and at depth. We show here that this relationship is far more irregular than previously suggested, and that it is not possible to simply correlate the increase of the slab dip to the increasing age of the downgoing cooler lithosphere. Younger oceanic lithosphere may show steeper dip than older segments of slabs (e.g., Central America vs. South America), in contrast with predictions of models considering only slab pull. The combination of slab age and subduction rate better accounts for slab dip; however the correlation is not satisfactory (correlation coefficient equal to 0.450). These results suggest that supplemental forces or constraints have to be accounted for, such as thickness and shape of the hangingwall plate, absolute plate velocity, presence of lateral density variations in the hosting upper mantle, effects of accretion/erosion, subduction of oceanic plateaus and slab deformation due to the motion of the mantle relative to the subducting plate.

Keywords: subduction zones; slab dip; lithospheric age; plate tectonics

1. Introduction

During the last 20 yr, the idea that the slab pull is primarily driving plate tectonics [1,2] has dominated our view of subduction. This stems from the fact that the cooler subducting lithosphere is heavier than the underlying mantle and it is assumed to drag the attached plate. This is consistent with the observation that plate motions are faster where there are longer subduction zones [3].

It has been demonstrated that the dip for a rigid slab would be controlled by a balance between the downward torque on the slab due to the weight of the slab and the upward torque on the slab due to the hydrodynamic forces from the induced corner flow in the viscous mantle surrounding the slab [4,5]. These

* Corresponding author. Department of Earth Sciences, University of Roma 'La Sapienza', Italy.
E-mail address: eugenio.carminati@uniromal.it (E. Carminati).

0012-821X/$ - see front matter © 2005 Published by Elsevier B.V.
doi:10.1016/j.epsl.2005.07.025

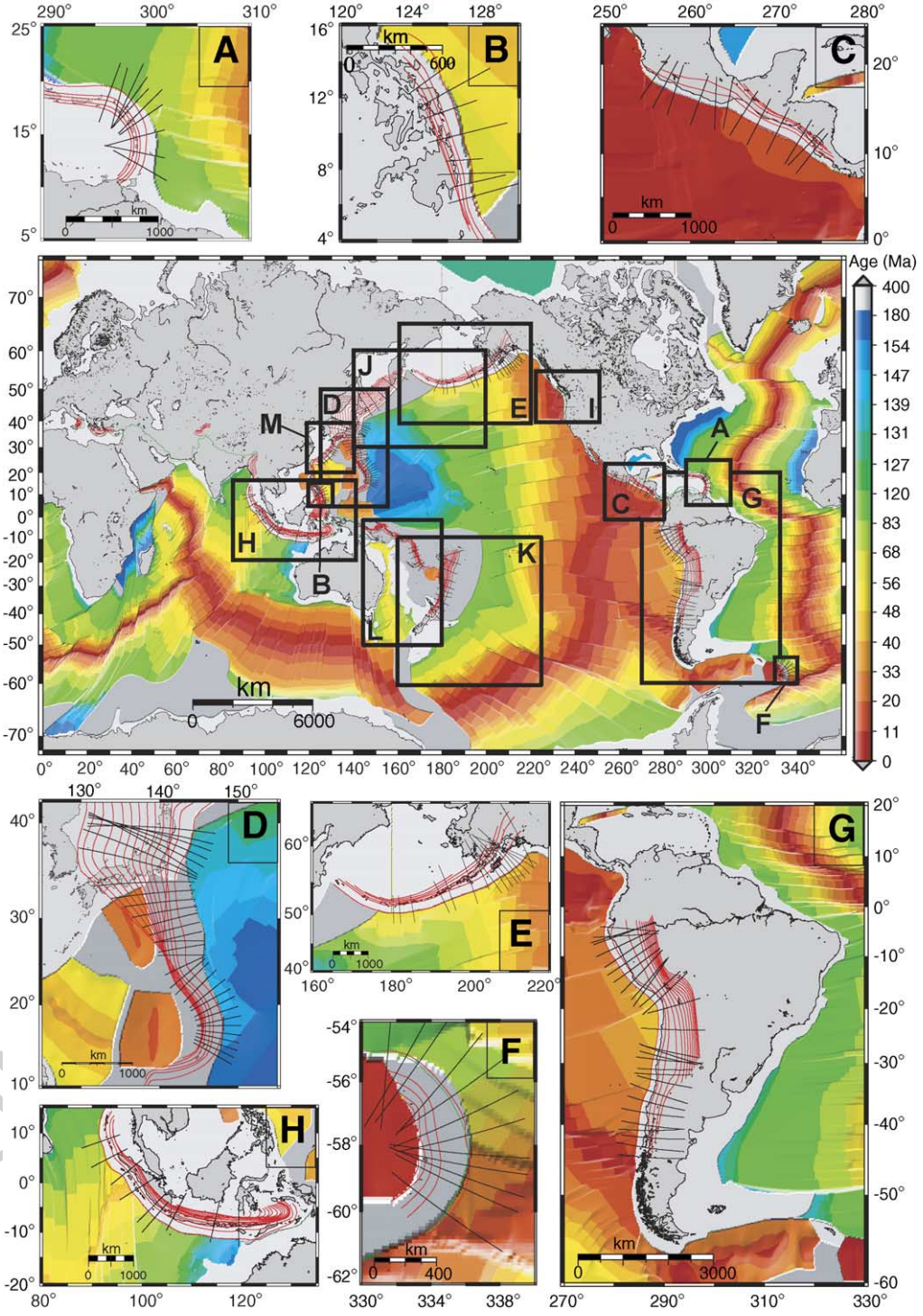
A
B
C
D
E
F
G
H
I
J
K
L
M
km
Age (Ma)
400
180
154
147
139
131
127
120
83
68
56
48
40
33
20
11
0

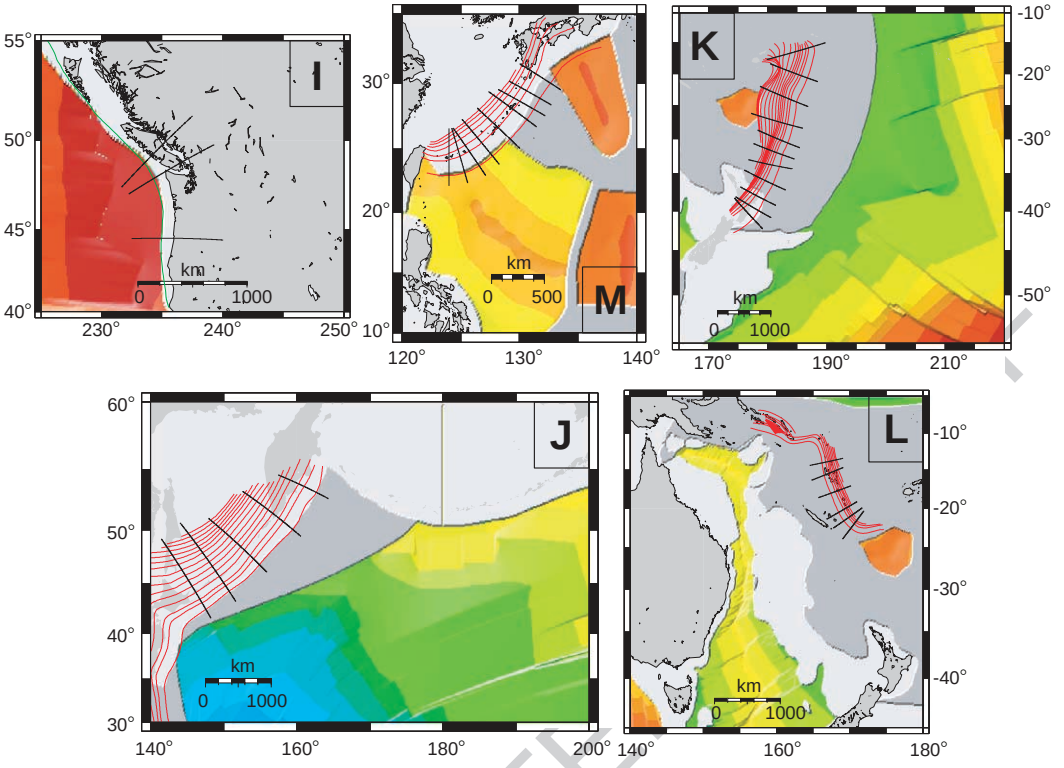

Fig. 1. Traces of the analyzed trench-perpendicular cross sections. The plate ages [15] and the extent of slabs described by the RUM project [10] are shown. Red isolines of the top of the slabs drawn every 100 km. Panels A–M show enlargements of analyzed subduction zones: (A) Caribbean; (B) Philippines; (C) Central America; (D) Marianas–Japan; (E) Eastern-Central Aleutins; (F) Sandwich arc; (G) South America; (H) Indonesia; (I) Cascades; (J) Kuril; (K) Tonga–Kermadec; (L) New Hebrides; (M) Ruykyu.

authors concluded that, because the buoyancy of the slab is proportional to its age, the dip of slabs composed of younger seafloor would be shallower. Such a view was shared by other studies, generally considering only the South America subduction zone [6–8]. Performing a statistical study on the factors controlling subduction zone geometry, considering subduction zones worldwide, Jarrard [9] concluded that the correlation between slab age and dip is negligible. Notwithstanding this conclusion, in Earth sciences literature it is still widely accepted that old and heavy (i.e., characterized by larger negative buoyancy) oceanic lithosphere exerts a larger down pull and thus determines a steeper slab dip.

The results of the pioneer study of Jarrard [9] had no later systematic control. Although the ages of ocean floor were well known in the mid-1980s, the deep geometry of subducting slabs was less constrained. Geophysical techniques, mostly tomography and seismological studies, have greatly improved our knowledge on mantle geometry since Jarrard's [9] study. Recently, the Regionalized Upper Mantle project (RUM; [10]) provided a worldwide image of subducting slabs, which constitutes a uniform database to check the results of Jarrard [9]. We performed this check on the 13 subduction zones shown in Fig. 1. The results exposed in this work do not support the scenario of a direct age control on the slab dip, in agreement with Jarrard's [9] findings.

2. Data and method

The following 13 subduction zones were considered: Caribbean, Philippines, Central America, Marianas–Japan, Eastern-Central Aleutins, Sandwich arc, South America, Indonesia, Cascades, Kuril, Tonga–Kermadec, New Hebrides, Ruykyu (Table 1). For the

t1.1 Table 1
t1.2 List of subduction zones and data analyzed in this study

t1.3 Subduction zone	Number of sections	Quality and provenance of slab dip data	Quality and provenance of slab age data	Availability of slab age at depth
t1.4 Caribbean	10	High; [10]	High; [15]	Yes
t1.5 Philippines	8	High; [10]	High; [15]	Yes
t1.6 Central America	12	High; [10]	High; [15,16]	Yes
t1.7 Marianas–Japan	32	High; [10]	High; [15,17]	Yes
t1.8 Aleutins	17	High; [10]	High; [15]	Yes
t1.9 Sandwich Arc	12	High; [10]	High; [15]	Yes
t1.10 South America	30	High; [10]	High; [15]	Yes
t1.11 Indonesia	9	High; [10]	High; [15]	Yes
t1.12 Cascades	3	Low; [14]	High; [15]	Yes
t1.13 Kuril	5	High; [10]	Low; manual extrapolation from [15]	No
t1.14 Tonga–Kermadec	11	High; [10]	Low; manual extrapolation from [15]	No
t1.15 New Hebrides	6	High; [10]	Low; [18]	No
t1.16 Ruykyu	9	High; [10]	Low; manual extrapolation from [15]	No

first eight subduction zones both ocean floor ages at the trench and detailed information on slab geometry are available. In the Cascades the geometry of the slab is only poorly known due to the lack of subcrustal seismicity but the knowledge of the age of the lithosphere entering the trench is precise. For the latter 4 subduction zones the slab geometry constraints are good, whereas the age constraints are rather loose.

Other subduction zones, such as the Aegean and the Italian arcs, had to be neglected due to the complete lack of age constraints. Subduction zones where continental collision occurred, such as Ontong Java, were also neglected. Finally we excluded subduction zones with trenches parallel to plate convergence, such as the Western Aleutins and Western Indonesia.

All the data acquired for the 13 subduction zones are provided in 26 tables as Background Data Set.

2.1. Slab dip

Using the GMT software [11] we constructed 164 mantle-scale cross sections of the slabs subducting in the 13 subduction zones (Fig. 1).

The sections shown in Fig. 1 are perpendicular to the trench (as in [9]). This allowed the measurement of the true dip of the slabs. This choice is justified by the fact that, in the case of convergence oblique to the trench, the strain is partitioned in trench-parallel and trench-perpendicular components (e.g., [12] and references therein for Central America). For most of the sections the angle between the section trace and the plate convergence vector is less than 45°. For only 22 sections (indicated by black squares rather than by circles in Fig. 4) this angle is between 45° and 67°.

At the same trench locations the slab dip was also measured along sections parallel to the plate convergence vector. It is emphasized however that such measures provide apparent dips, constantly lower than the true dip. The difference between apparent and true dip increases with the angle between the plate convergence and the trench-perpendicular direction.

The slab geometries used are those provided by the RUM project (http://wwwrses.anu.edu.au/seismology/projects/RUM; [10]), built on contouring of slab-related seismicity from the relocated catalogue of Enghdal et al. [13] and of the International Seismological Centre catalog (http://www.isc.ac.uk). The contours (Fig. 1) trace the top of slabs occurring worldwide. Only for the Cascades subduction zone, not considered by the RUM project, information on the shallow portions of the slab were taken directly from earthquakes reported in the Enghdal et al. [1998] catalogue whereas the dip of the slab at depths deeper than 50 km was taken from a local tomography study [14].

Average slab dips were measured, when possible, for the following depth ranges: 0–50, 50–100, 100–150, 150–200, and 200–250 km. The average (from 0 to 250 km depth) dip D_{av} was also calculated. The slab dips were plotted either against the age of the lithosphere entering the subduction zone (Figs. 2 and 3) or either against distance (in km) parallel the sub-

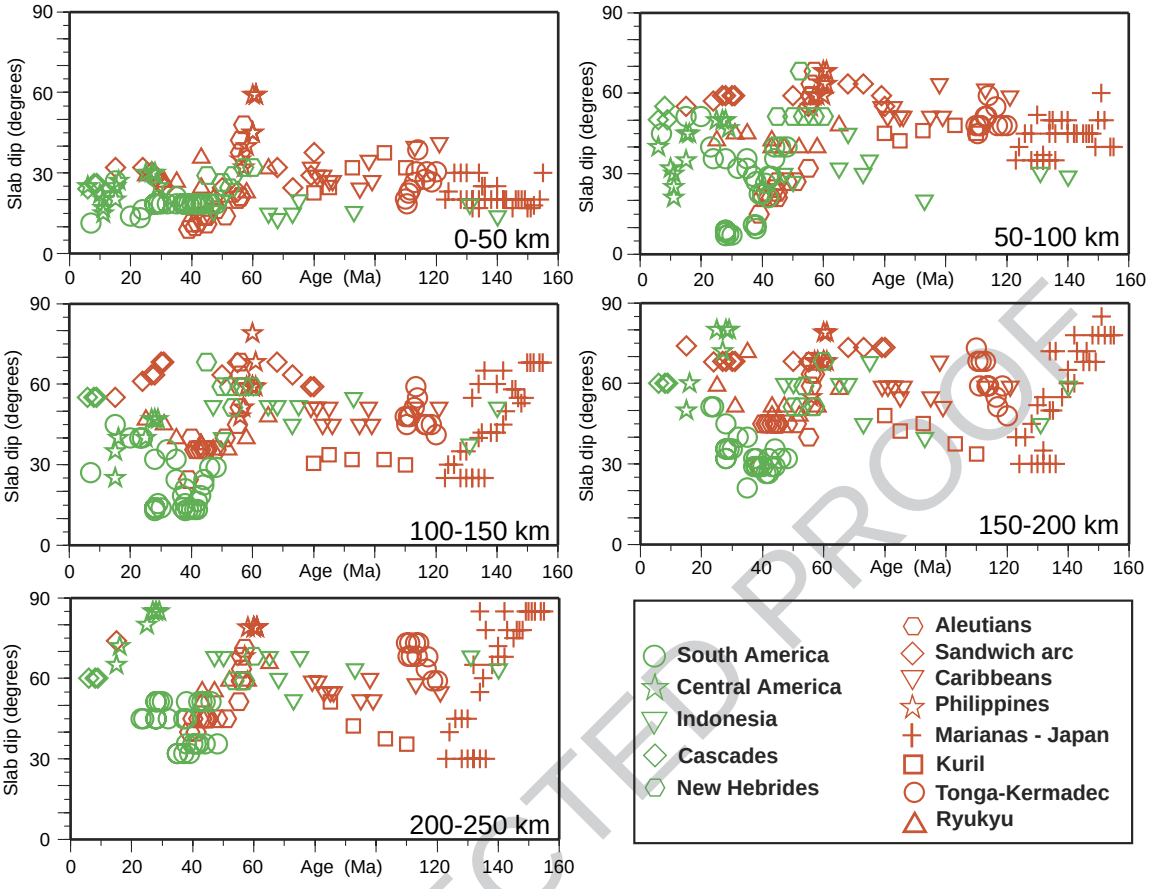

Fig. 2. Age vs. slab dip plots for 5 different depth ranges, with data measured along sections perpendicular to the trench.

duction zone (Figs. 4 and 5). In these latter graphs, the age of the subducting lithosphere has been also plotted so to check the dip–age relationship.

2.2. Slab age

The plate ages (A_t) of the oceanic lithosphere entering nine subduction zones (Caribbean, Philippines, Central America, Marianas–Japan, Eastern-Central Aleutins, Sandwich arc, South America, Indonesia, Cascades) were taken from the GMT globalage_1.6.grd file, based on the work by Mueller et al. [15], which was integrated with data from Protti et al. [16] for the Central America zone and from Nakanishi et al. [17] for the Japan zone.

For the Kuril, Tonga–Kermadec and northern Ruykyu subduction zones no information on the age of the lithosphere entering the trench is provided by the Mueller et al. [15] database. Following Heuret and Lallemand [18], the ages at these trenches are extrapolated from the nearest magnetic anomalies. For the New Hebrides we adopt the ages reported in [18]. Such a procedure, however, introduces a wealth of arbitrariness in the measurements and the ages have to be considered with caution.

For nine subduction zones (Caribbean, Central America, South America, Philippines, Marianas–Japan, Indonesia, Eastern-Central Aleutins, Sandwich Arc, Cascades) we calculated the age of the slab at various depths (50, 100, 150, 200, 250 km) using the same relationship of Jarrard [19,9]: $A_d = A_t + L(dA/dL - 1/V_s)$, where A_d is the age at depth, A_t is the age of the lithosphere entering the trench, V_s is the velocity of subduction (i.e., convergence rate plus eventual backarc opening; see next section), L is the length of the slab from the trench to the considered depth and

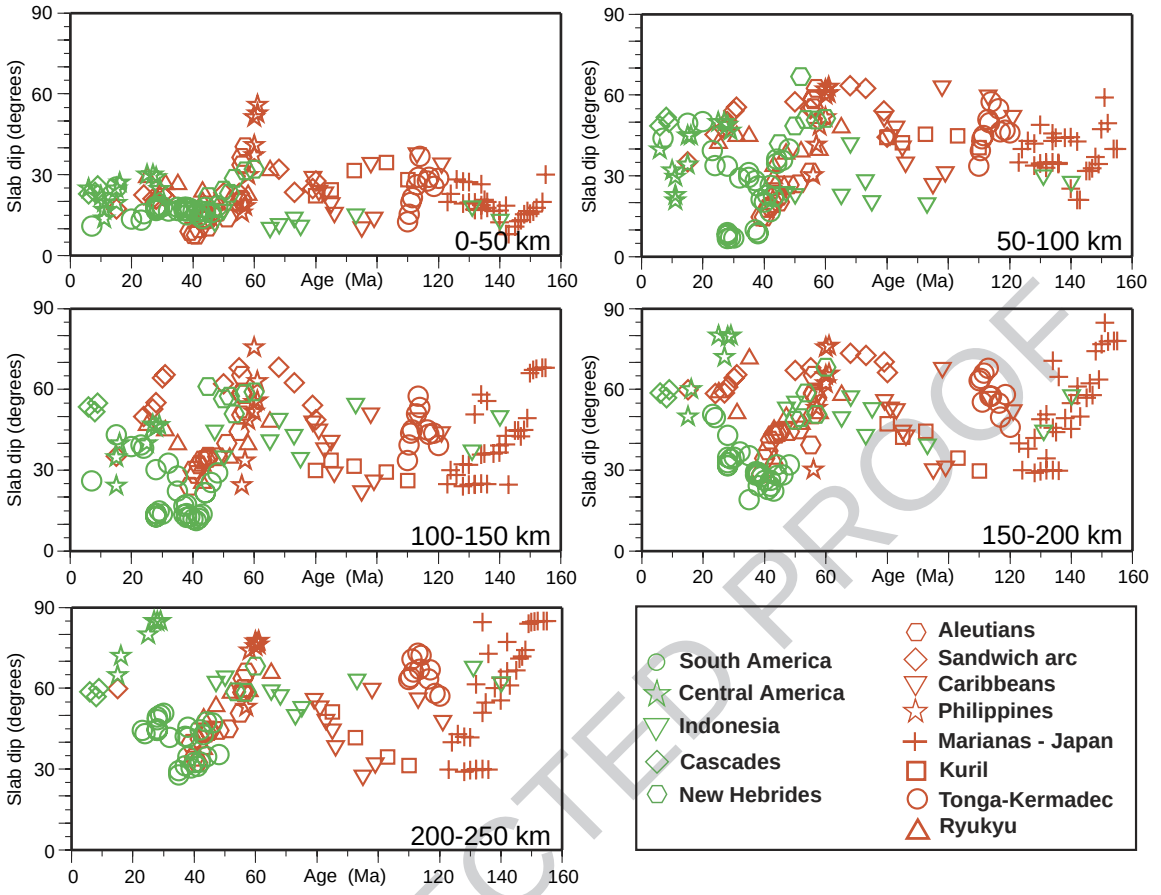

Fig. 3. Age vs. slab dip plots for 5 different depth ranges, with data measured along sections parallel to the plate convergence vector.

dA/dL is the age gradient of the slab, measured in the lithosphere approaching the trench. The age gradient dA/dL is averaged over a distance of 250 km from the trench parallel to the convergence vector. The calculated age is not the present age of the slab at the considered depth, but rather the age of that part of the slab when it first entered the subduction zone.

The choice of limiting the age calculation to these nine subduction zones is due to the fact that only for these zones direct information on the age of the lithosphere entering the trench is available. For the four remaining subduction zones the calculation of dA/dL without precise age information for the lithosphere approaching the trench would have been extremely speculative.

There is a high degree of uncertainty of the age-at-depth calculation procedure. The uncertainty mainly derives from the determination of dA/dL, clearly controlled by the crossing of transform faults, especially in zones where transforms are markedly oblique to the convergence vector (e.g., South America, Sandwich and Caribbean subduction zones). Moreover, the age gradient at depth could be different from that of the lithosphere approaching the trench and the constraints on the velocity of backarc opening are usually quite loose. Finally, the velocity of convergence and backarc opening may largely vary through time (e.g., the backarc opening of the Marianas [20]).

2.3. Subduction velocity

For each profile, the convergence velocity V_c (both azimuth and magnitude) was calculated using the

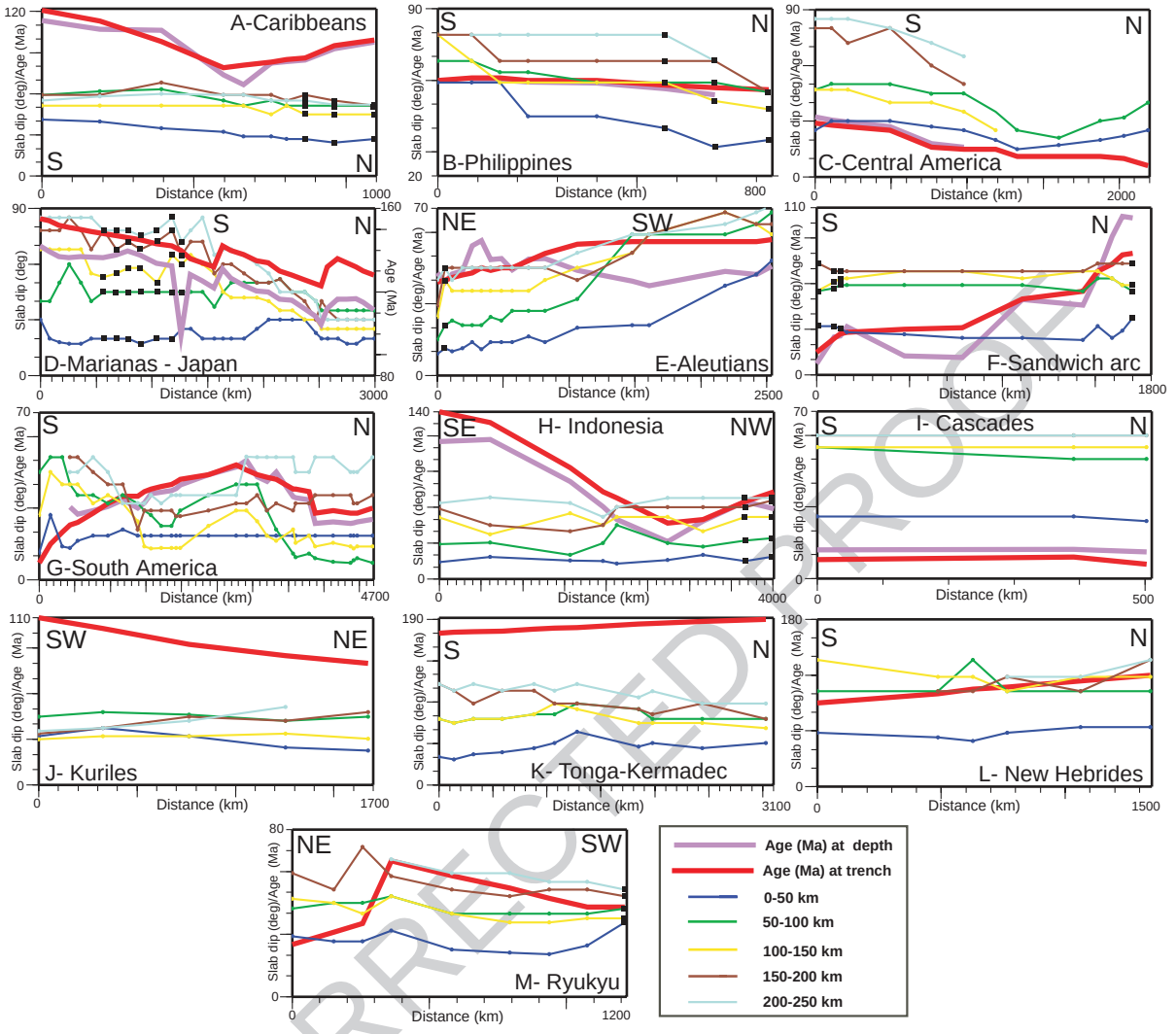

Fig. 4. Distance (along the subduction zone) vs. slab dip plots for the 13 analyzed subduction zones. Data were measured along sections perpendicular to the trench. The age (Myr) of the lithosphere entering the trench (At) is plotted. The age of the subducted lithosphere at depth is also plotted for 9 subduction zones. Normally the considered slab depth is 250 km (A250 is plotted; see Supplemental material), with the exception of the Sandwich Arc, where the depth is 200 km (A200 is plotted). Notice that for the Marianas–Japan zone, the scales of slab dip and age are different. The black squares label sections where the angle between the section trace and the plate convergence vector is larger than 45°.

rotation poles of the NUVEL1A model [21]. No plate convergence estimates are provided for the New Hebrides subduction zone, because no information on the velocity of the subducting plate is available from the NUVEL1A model. The component of convergence rate parallel to the sections was also calculated. The velocity of backarc opening V_b was evaluated from the literature in order to calculate the subduction velocity V_s that enters the calculation of the age at depth. V_s is equal to V_c+V_b (i.e., convergence rate plus, possibly, backarc opening). $V_b=20$ mm/yr is evaluated for the Caribbean [22] and $V_b=50$ mm/yr for the Sandwich arc [23]. V_b in the backarc of the Marianas subduction varies from 20 mm/yr in the northern part to 47 mm/yr in the south [20]. A progressive linear increase between the two rates is assumed for the Marianas sections. The backarc opening of the Japan subduction is inactive [24] and the

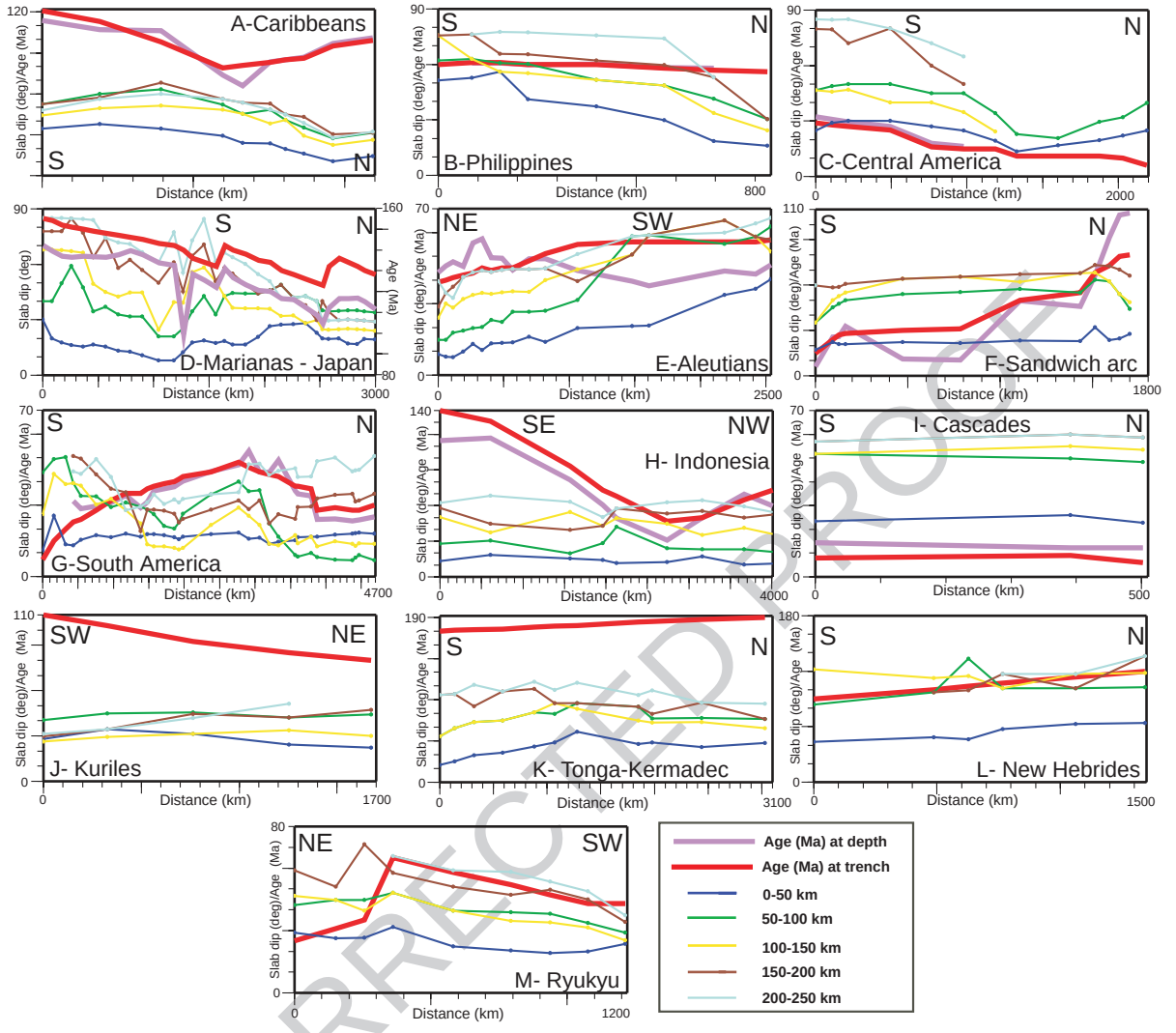

Fig. 5. Distance (along the subduction zone) vs. slab dip plots for the 13 analyzed subduction zones. Data were measured along sections parallel to plate convergence. The age (Myr) of the lithosphere entering the trench (At) is plotted. The age of the subducted lithosphere at depth is also plotted for 9 subduction zones. Normally the considered slab depth is 250 km (A250 is plotted; see Supplemental material), with the exception of the Sandwich Arc, where the depth is 200 km (A200 is plotted). Notice that for the Marianas–Japan zone, the scales of slab dip and age are different.

backarc area is subject to shortening rather than to extension. $V_b = -25$ mm/yr [25] is used in our calculations for the Japan subduction. For the Tonga–Kermadec a V_b of 160 mm/yr is assumed, as measured in the Lau basin [26].

Along the Indonesian subduction zone, backarc extension is localized in the northwestern segment of the arc, i.e., in the Andaman Sea [27], where about 3 mm/yr of N–S extension are measured [28]. No backarc opening is observed in the remaining portions of the Indonesia subduction zone [28] and $V_b = 0$ is assumed for these areas. $V_b = 0$ is assumed also for Central America, South America, Cascades, Philippines because these subduction zones are not bordered by backarc basins [24]. Finally $V_b = 0$ is assumed for the Aleutins and Kuriles since they are bordered by a backarc basin inactive since the Cretaceous [24].

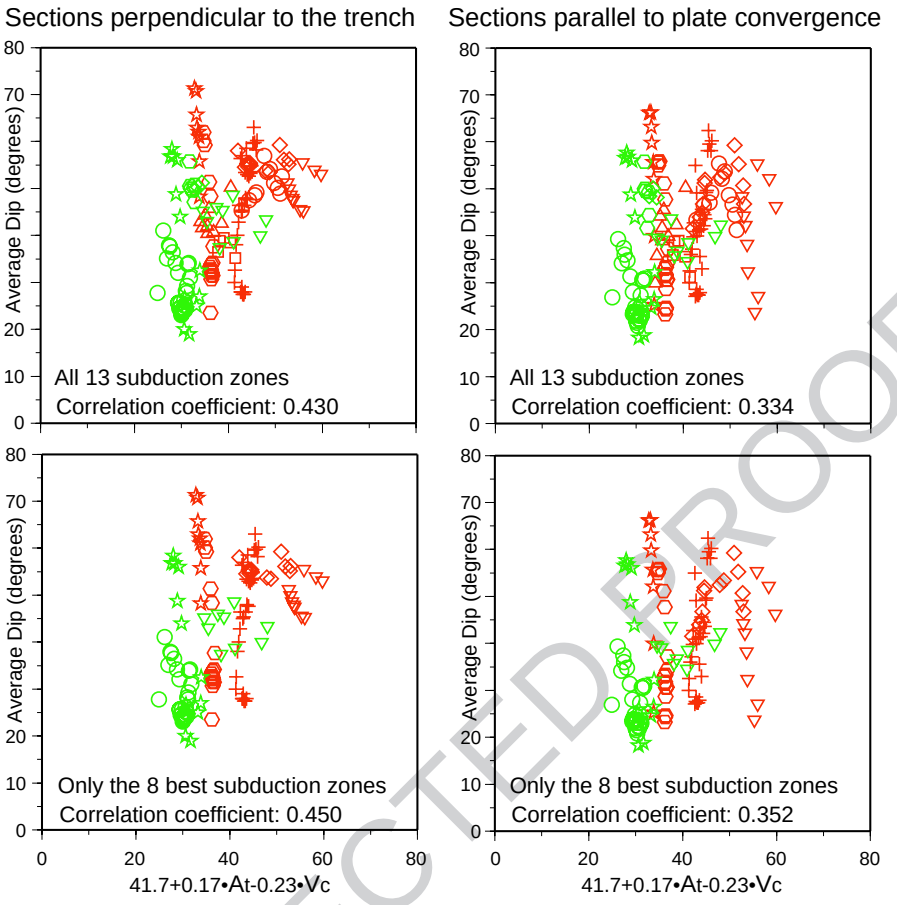

Fig. 6. Average dips are plotted against the results of the Jarrad's [9,19] relationship. The symbols are as in Figs. 2 and 3. Plots are shown for all the subduction zones (except the New Hebrides) and for the 8 best-constrained zones (Caribbean, Philippines, Central America, Marianas–Japan, Eastern-Central Aleutins, Sandwich arc, South America, Indonesia).

Convergence and backarc opening rates were utilized to calculate the slab age at depth. Moreover they were used to check the hypothesis that $D_{av}=41.7+0.17\cdot A_t-0.23\cdot V_c$ (Fig. 6). According to Jarrard [9,19] this empirical relationship provides the best correlation between dip, age and subduction velocity. Finally we consider the variations in slab dip as a function of the thermal parameter T (Fig. 7), calculated as the product of the slab vertical descend rate V_v and the age of subducting lithosphere: $T=V_v\cdot A_t$.

3. Results and discussion

The slab dip vs. age graphs for different depth ranges (Figs. 2 and 3 for trench-perpendicular and for convergence–parallel sections respectively) were produced to identify a worldwide relationship between age and slab dip. If a direct function between these two parameters existed, the plotted symbols should approximately follow an increasing trend. Such a trend is not recognized both at global scale or within single subduction zones. For example, at global scale the Marianas–Japan zone, although characterized by the oldest ages, shows slab dips comparable or lower to those of the youngest slab (Sandwich arc). A second worldwide result is that, at least in the 0–150 km depth range, west-directed zones (red symbols) generally show, for comparable slab ages, steeper geometries than east or northeast-directed zones (green symbols). However, a few notable exceptions occur, such as the New Hebrides slab showing dips

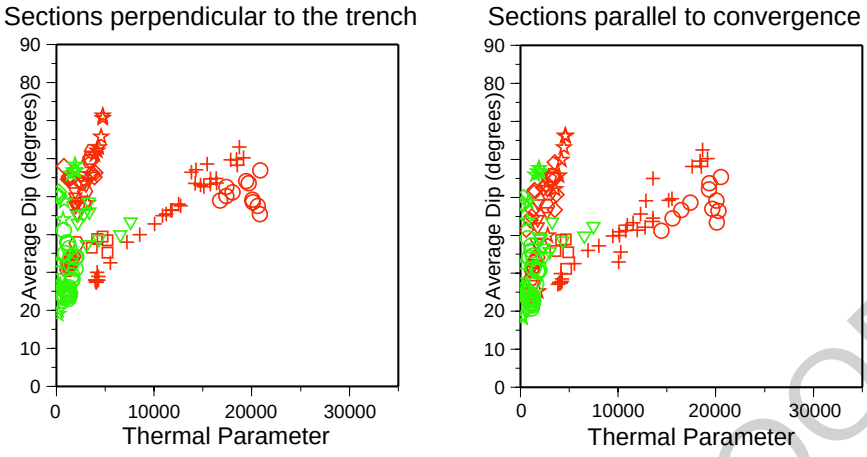

Fig. 7. Average dip is plotted against the thermal parameter. The symbols are as in Figs. 2 and 3. Plots are shown for all the subduction zones (except the New Hebrides) and for the 8 best-constrained zones (Caribbean, Philippines, Central America, Marianas–Japan, Eastern-Central Aleutins, Sandwich arc, South America, Indonesia).

comparable or steeper than the same-age west-directed zones. However, it has to be recalled that the age constraints for the New Hebrides subduction zones are quite loose. A second exception is provided by the Central America slab, which is steeper, in the 150–250 km range than the same-age west-dipping slabs.

Analysing single subduction zones in Figs. 2 and 3, increasing age–dip trends are not generally recognized, with the exception of the Marianas–Japan and E-Aleutians zones. On the contrary, a decreasing age–dip trend is recognized for the South America subduction in the 50–200 km depth interval and for the Kuril and Tonga–Kermadec (whose slab ages are however poorly constrained) subduction zones in the 150–250 km interval. Constant dip–age trends are recognized for the Indonesia, Sandwich Arc and Caribbean (constant in Fig. 2 and decreasing in Fig. 3) subduction zones. It is finally stressed that these considerations hold for both trench-perpendicular and convergence–parallel sections, because Figs. 2 and 3 differ only slightly.

Figs. 4 and 5 show the dip and age trends along trench of all the analyzed slabs for trench-perpendicular and for convergence–parallel sections respectively. Because Figs. 4 and 5 show very similar trends, although different in details, the following observations are valid for trench-perpendicular and for convergence–parallel sections. For nine sections, ages at the trench and at 250 km depth (with the exception of the Sandwich arc, where the considered depth is 200 km) are shown. The two ages generally show similar trends with the only exception of the Aleutians, where the trends are significantly different. Therefore the following considerations, if not specified, hold for age both at the trench and at depth. The trends of ages at depth are generally smooth and mimic the trends of ages at the trench. Singularities, such as at 1270 km distance in the Marianas–Japan or at 2900 and 3300 km distances in the South America panels, are due to measurements of anomalous age gradients along sections crossing transform faults.

It is immediately noted that the slab dip does not necessarily increase steadily with depth, as for example in the Central America, South America, Marianas–Japan, Caribbean, Kuril, Tonga–Kermadec, New Hebrides and Ryukyu subduction zones. This observation seems to contradict the prediction of slab pull models. A downpull should, as a matter of fact, determine a steady increase of dip with depth [29,30]. The observed irregular shape of the subducting slabs appears to be controlled by other factors. A potential candidate for the upper 250 km could be the shape and thickness of the overriding plate. Oblique and lateral subduction zones with respect to the direction of convergence show generally steeper slabs (e.g. in central Southern America).

In the South America subduction zone, slab dip is direct function of age only for the central sector of the

subduction zone, whereas in the southern part an inverse function is displayed. An overall direct function of age at the trench and dip occurs in the Eastern Aleutians, whereas in the Central Aleutians (i.e. for distances greater than 1000 km) dips increase while age at the trench remains constant. The age at 250 km depth slightly diminishes from east to west. Therefore, an inverse function occurs between age at depth and slab dip. In the Sandwich arc no increase of slab dip corresponds to a pronounced south to north increase of slab age. In Central America, the slab dip is direct function of age only in the southern part, whereas in the northern part a slight decrease of age corresponds to an increase of dip. In the Philippines a constant slab age is accompanied by a decrease of slab dip from north to south for most of the depth ranges. The pattern in the Marianas–Japan subduction is more complicated. A general decrease of slab age from south to north is generally accompanied by a decrease of slab dip. However, exceptions to this rule are observed in the southern part. The Caribbean subduction zone shows minimum slab ages in the central part and a significant increase of age both to the N and to the S, while the slab dip is fairly constant throughout the entire subduction zone. The south Indonesia subduction zone also shows rather constant slab dips that are not direct function of the slab age, which decreases from the NW and SE edges of the subduction zone towards the center. The Cascades and New Hebrides subduction zones show constant age trends and corresponding constant dip trends. In the Kuriles, age is constantly and significantly decreasing (some 35 Myr) from SW to NE, whereas dips remain quite constant. In the Tonga–Kermadec subduction, a slight increase of age (ca. 10 Myr) is not matched by the slab dip, which shows a decreasing trend, if any. Finally in the NE part of the Ryukyu subduction zone, a 40 Myr increase of age does not correspond any significant slab dip variation.

In summary, seven subduction zones (Sandwich arc, Philippines, Caribbean, Indonesia, Kuriles, Tonga–Kermadec and Ryukyu) show geometries that are opposite to those predicted by slab pull models, three (Marianas–Japan, Cascadia and New Hebrides) show consistent geometries and the remaining two (South America and Central America) show intermediate characters. Finally, the Aleutins show intermediate character when the age at trench is considered and a character similar to the first seven zones when age at 250 km depth is considered.

In Fig. 6 the average dips are plotted against the results of the Jarrard's [9,19] relationship $41.7+0.17 \cdot A_t - 0.23 \cdot V_c$ and the corresponding correlation coefficients are provided. The New Hebrides subduction was excluded from these calculations because no information on the convergence rate is available. If the relationship were valid, the symbols should align along a line at 45° starting from the origin. In Fig. 6 the data are quite scattered indicating that the relationship is not valid for the new data here presented. This is confirmed by the low correlation coefficients. The largest value (0.450) is far lower than the value (0.717) obtained by Jarrard [9,19]. It has to be noted that Jarrard [9,19] himself doubted the validity of the relationship, suggesting that the obtained high correlation coefficient may only be a coincidence.

Finally, in Fig. 7 we plot average dip against thermal parameter ($T = V_v \cdot A_t$; once again the New Hebrides subduction is excluded). This latter value is a simple way of estimating the overall temperature structure of the deep slab (i.e., larger thermal parameters correspond to cooler slab temperatures) and it is normally correlated to the maximum depth of seismicity within slabs. When all the data are considered, the correlation between slab dip and thermal parameter is weak. However two major trends can be recognized. The first is steeper and comprises most of the subduction zones. The second is less steep and is made by data from the Marianas–Japan and Tonga–Kermadec subduction zones. This seems to indicate a thermal control on slab dip, i.e., cooler slabs may be steeper. Theoretically a thick old slab is more dense but, at the same time, stiffer and harder to bend. Fig. 7 suggests that the effect of temperature on density prevails on its effect on rheology. However, slab buoyancy at depth does not simply depend on age and subduction velocity, but it is influenced by lithosphere warming and phase changes.

4. Conclusions

The evidence presented in this paper casts some doubt on the effectiveness of the slab pull, as indi-

cated also by the down-dip compression occurring in several slabs [31,32].

A simple linear relation between slab dip and age of the downgoing oceanic lithosphere does not exist. A combination of slab age and subduction velocity correlates better with slab dip, but is still not satisfactorily (correlation coefficient equal to 0.450). These results suggest that supplemental forces to the negative buoyancy of the slab have to be considered. Plate kinematics (absolute motion of upper plate [33,34]) could play a role, but other aspects have to be taken into account. The first one is the presence of lateral density variations in the hosting upper mantle, allowing different buoyancy contrasts with the downgoing slab. However, apart from proven lateral heterogeneities in mantle tomography, there is no evidence yet for such large anisotropies in composition in order to justify sufficient density anomalies in the upper mantle. The effect of latent heat released by phase transitions could, moreover, alter the thermal distribution and buoyancy of subducting slabs and control their dips [35]. Another parameter possibly controlling the dip of the first 250 km could be the thickness and shape of the hangingwall plate, i.e., the thicker the hangingwall plate, steeper the slab. Still at shallow depths, the effects of accretion/erosion [36,37], the thickness of sediments in the trench and the subduction of oceanic plateaus [38] could influence the geometry of the descending lithosphere. Another basic controlling factor could be operated by resistance forces induced by the motion of the mantle relative to the subducting plate [39,40]. According to Hager and O'Connell [41] the dip of the subduction zones is controlled by the return flow of the mantle produced by the plate motion rather than by slab density contrast. The lack of a clear correlation between the observed dip angle of slabs and plate velocity and slab age in modern subduction zones has been explained with the hypothesis that subduction is a time-dependent phenomenon [42].

Acknowledgements

Research supported by 'La Sapienza' University. The suggestions of two anonymous reviewers and of the editor (Scott King) greatly improved the quality of this work. Marco Cuffaro is warmly thanked for help with plate velocity calculations.

Appendix A. Supplementary data

Supplementary data associated with this article can be found, in the online version, at doi:10.1016/j.epsl.2005.07.025.

References

[1] D.L. Anderson, Topside tectonics, Science 293 (2001) 2016–2018.
[2] C.P. Conrad, C. Lithgow-Bertelloni, How mantle slabs drive plate tectonics, Science 298 (2003) 207–209.
[3] D. Forsyth, S. Uyeda, On the relative importance of driving forces of plate motion, Geophys. J. R. Astron. Soc. 43 (1975) 163–200.
[4] D.J. Stevenson, J.S. Turner, Angle of subduction, Nature 270 (1977) 334–336.
[5] A. Tovish, G. Schubert, B.P. Luyendyk, Mantle flow pressure and the angle of subduction; non-Newtonian corner flows, J. Geophys. Res. 83 (1978) 5892–5898.
[6] M.J.R. Wortel, N.J. Vlaar, Age-dependent subduction of oceanic lithosphere beneath western South America, Phys. Earth Planet. Inter. 17 (1978) 201–208.
[7] M. Barazangi, B.L. Isacks, Subduction of the Nazca plate beneath Peru: evidence from spatial distribution of earthquakes, Geophys. J. R. Astron. Soc. 57 (1979) 537–555.
[8] T.E. Jordan, B.L. Isacks, R.W. Allmendinger, J.A. Brewer, V.A. Ramos, C.J. Ando, Andean tectonics related to the geometry of the subducted Nazca plate, Geol. Soc. Amer. Bull. 94 (1983) 341–361.
[9] R.D. Jarrard, Relations among subduction parameters, Rev. Geophys. 24 (1986) 217–284.
[10] O. Gudmundsson, M. Sambridge, A Regionalized Upper Mantle (RUM) seismic model, J. Geophys. Res. 103 (1998) 7121–7136.
[11] P. Wessel, W.H.F. Smith, New version of the generic mapping tools released, EOS 76 (1995) 329.
[12] J.J. Martinez-Díaz, J.A. Alvar-Gomez, B. Benito, D. Hernandez, Triggering of destructive earthquakes in El Salvador, Geology 32 (2004) 65–68.
[13] E.R. Engdahl, R.D. van der Hilst, R.P. Buland, Global teleseismic earthquake relocation with improved travel times and procedures for depth determination, Bull. Seismol. Soc. Am. 88 (1998) 722–743.
[14] M.G. Bostock, J.C. VanDecar, Upper mantle structure of the northern Cascades subduction zone, Can. J. Earth Sci. 32 (1995) 1–12.
[15] R.D. Mueller, W.R. Roest, J.Y. Royer, L.M. Gahagan, J.G. Sclater, Digital isochrons of the world's ocean floor, J. Geophys. Res. 102 (1997) 3211–3214.

[16] M. Protti, F. Gundel, K. McNally, Correlation between the age of the subducting Cocos plate and the geometry of the Wadati–Benioff zone under Nicaragua and Costa Rica, Spec. Pap. - Geol. Soc. Am. 295 (1995) 309–326.
[17] M. Nakanishi, K. Tamaki, K. Kobayashi, Mesozoic magnetic anomaly lineations and seafloor spreading history of the Northwestern Pacific, J. Geophys. Res. 94 (1989) 15437–15462.
[18] A. Heuret, S. Lallemand, Plate motions, slab dynamics and back-arc deformation, Phys. Earth Planet. Inter. 149 (2005) 31–51.
[19] R.D. Jarrard, Prediction of continental structural style from plate tectonic parameters, EOS Trans. AGU 65 (1984) 1095.
[20] T. Yamazaki, N. Seama, K. Okino, K. Kitada, M. Joshima, H. Oda, J. Naka, Spreading process of the northern Mariana Trough: rifting–spreading transition at 22° N, Geochem. Geophys. Geosyst. 4 (2003) 1075, doi:10.1029/2002GC000492.
[21] C. De Mets, R.G. Gordon, D.F. Argus, S. Stein, Effect of recent revisions to the geomagnetic reversal time scale on estimates of current plate motions, Geophys. Res. Lett. 21 (1994) 2191–2194.
[22] J.C. Weber, T.H. Dixon, C. DeMets, W.B. Ambeh, P. Jansma, G. Mattioli, J. Saleh, G. Sella, R. Bilham, O. Pérez, GPS estimate of relative motion between the Caribbean and South American plates, and geologic implications for Trinidad and Venezuela, Geology 29 (2001) 75–78.
[23] P.F. Barker, I.A. Hill, Back-arc extension in the Scotia Sea, Philos. Trans. R. Soc. Lond. Ser. A: Math. Phys. Sci. 300 (1981) 249–262.
[24] W.P. Schellart, G.S. Lister, Tectonic models for the formation of arc-shaped convergent zones and backarc basins, in: A.J. Sussman, A.B. Weil (Eds.), Orogenic Curvature: Integrating Paleomagnetic and Structural Analyses, Geological Society of America Special Paper, vol. 383, 2004, pp. 237–258.
[25] K. Shimazaki, Y. Zhao, Dislocation model for strain accumulation in a plate collision zone, Earth Planets Space 52 (2000) 1091–1094.
[26] M. Bevis, F.W. Taylor, B.E. Schutz, J. Recy, B.L. Isacks, S. Helu, R. Singh, E. Kendrick, J. Stowell, B. Taylor, S. Calmant, Geodetic observations of very rapid convergence and back-arc extension at the Tonga arc, Nature 374 (1995) 249–251.
[27] R. Hall, The plate tectonics of Cenozoic SE Asia and the distribution of land and sea, in: R. Hall, J.D. Holloway (Eds.), Biogeography and Geological Evolution of SE Asia, Backbuys Publishers, Leiden, The Netherlands, 1998.
[28] C. Kreemer, W.E. Holt, A.J. Haines, An integrated global model of present-day plate motions and plate boundary deformation, Geophys. J. Int. 154 (2003) 8–34.
[29] A.I. Shemenda, Subduction of the lithosphere and back-arc dynamics: insights from physical modeling, J. Geophys. Res. 98 (1993) 16167–16185.
[30] R. Hassani, D. Jongmans, Study of plate deformation and stress in subduction processes using two-dimensional numerical models, J. Geophys. Res. 102 (1997) 17951–17965.
[31] B. Isacks, P. Molnar, Distribution of stresses in the descending lithosphere from a global survey of focal-mechanism solutions of mantle earthquakes, Rev. Geophys. 9 (1971) 103–174.
[32] A. Frepoli, G. Selvaggi, C. Chiarabba, A. Amato, State of stress in the Southern Tyrrhenian subduction zone from fault–plane solutions, Geophys. J. Int. 125 (1996) 879–891.
[33] B.P. Luyendyk, Dips of downgoing lithospheric plates beneath island arcs, Geol. Soc. Amer. Bull. 81 (1970) 3411–3416.
[34] A. Tovish, G. Schubert, Island arc curvature, velocity of convergence and angle of subduction, Geophys. Res. Lett. 5 (1978) 329–332.
[35] J. van Hunen, A.P. van den Berg, N.J. Vlaar, Latent heat effects of the major mantle phase transitions on low-angle subduction, Earth Planet Sci. Lett. 190 (2001) 125–135.
[36] D.E. Karig, J.G. Caldwell, E.M. Parmentier, Effects of accretion on the geometry of the descending lithosphere, J. Geophys. Res. 81 (1976) 6281–6291.
[37] S.E. Lallemand, P. Schnurle, S. Manoussis, Reconstruction of subduction zone paleogeometries and quantification of upper plate material losses caused by tectonic erosion, J. Geophys. Res. 97 (1992) 217–239.
[38] T.A. Cross, R.H. Pilger, Controls of subduction geometry, location of magmatic arcs, and tectonics of arc and back-arc regions, Geol. Soc. Amer. Bull. 93 (1982) 545–562.
[39] C.H. Scholz, J. Campos, On the mechanism of seismic decoupling and back arc spreading at subduction zones, J. Geophys. Res. 100 (1995) 22103–22115.
[40] C. Doglioni, P. Harabaglia, S. Merlini, F. Mongelli, A. Peccerillo, C. Piromallo, Orogens and slabs vs. their direction of subduction, Earth Sci. Rev. 45 (1999) 167–208.
[41] B.H. Hager, R.J. O'Connell, Subduction zone dip angles and flow driven by plate motion, Tectonophysics 50 (1978) 111–133.
[42] S.C. King, Subduction zones: observations and geodynamic models, Phys. Earth Planet Inter. 127 (2001) 9–24.